BIOPOLYMERS VOL. 16, 157–185 (1977)

Ion Complexation in Nonactin, Monactin, and Dinactin: A Raman Spectroscopic Study

IRVIN M. ASHER,* GEORGE D. J. PHILLIES,† B. J. KIM,‡ and H. E. STANLEY,‡ *Harvard–M.I.T. Program in Health Sciences and Technology and Department of Physics, Massachusetts Institute of Technology, Cambridge, Massachusetts 02139*

Synopsis

The ability of the macrotetrolide nactins to complex selectivity with a wide variety of cations makes these ionophorous antibiotics important model systems for the study of biologic ionic transport. We report a Raman spectroscopic investigation of the Na^+, K^+, Rb^+, Cs^+, Tl^+, NH_4^+, NH_3OH^+, $C(NH_2)_3^+$, and Ba^{++} complexes of nonactin, monactin, and dinactin in 4:1 (v/v) $CH_3OH/CHCl_3$ and in the solid state. The nactins display characteristic spectral changes upon complexation, some of which are specific for a given cation. In the K^+, Rb^+, Cs^+, NH_3OH^+, and $C(NH_2)_3^+$ complexes, which are apparently isosteric, the ester carbonyl stretch frequency is found to be linearly proportional to the cation–carbonyl electrostatic interaction energy, as calculated from a simplified model. Deviations for the Na^+, NH_4^+, Tl^+, and Ba^{++} complexes are interpreted as arising from additional nonelectrostatic interactions. Additional information is obtained from other spectral regions and from measurements of depolarization ratios. Spectra of the nactin complexes differ from each other more in the solid state than in solution, reflecting the effects of crystalline contact forces.

INTRODUCTION

The macrotetrolide nactins [Fig. 1(a)] are a family of macrocyclic ionophorous antibiotics whose ability to complex, selectively, a wide variety of cations[1–3] has made them particularly interesting in the study of selective ion transport. In solution, the individual uncomplexed nactin molecules apparently adopt a relatively open, flat, flexible set of conformations.[3] However, upon complexation, the nactin molecule is believed to take on a single, relatively rigid conformation similar to that found in crystalline nactin complexes[4–7] [Fig. 1(b)]. The cation is located at the center of the complex, faced by the four ester and the four ether oxygen atoms. The remainder of the nactin molecule is so arranged that the complex presents a hydrophobic exterior to the solvent, which may explain the ability of the nactins to facilitate the extraction of ions into nonpolar solvents.

* Present address: Office of Science, HFS-50, U.S. Food and Lrug Administration, HEW, Rockville, Maryland 20852.

† Present address: Department of Chemistry, University of California Los Angeles, Los Angeles, California 90024.

‡ Present address: Department of Physiology, Boston University Medical School, Boston, Mass. 02118.

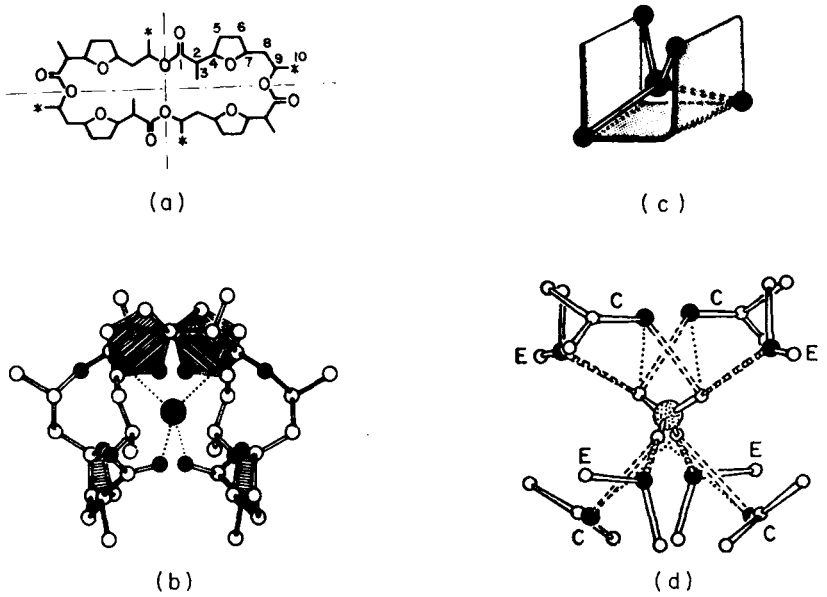

Fig. 1. (a) Chemical structure of nonactin. In monactin, one of the asterisked methyl groups is replaced with an ethyl group. There are two such replacements in dinactin, three in trinactin, and four in tetranactin. Carbon atoms are numbered for reference in text. (b) X-ray crystallographic structure of the nonactin–K^+ complex (after Ref. 5). (c) Simplified schematic drawing of the coordination of a cation to the ester carbonyl groups of nonactin, emphasizing the tetrahedral symmetry of the ester carbonyl groups. (d) Coordination and hydrogen bonding of NH_4^+ to the carbonyl (C) and tetrahydrofuran (E) oxygen atoms of tetranactin (after Ref. 7).

The available X-ray crystallographic data are summarized in Table I. In the nonactin–K^+ complex[5] [Fig. 1(b)], the cation is tetrahedrally coordinated [Fig. 1(c)] by the four ester carbonyl groups. The structure of crystalline nonactin–Na^+ complex[8] is found to be similar, although the internal cavity is found to be substantially larger than the Na^+ ion it contains. Similar structures are found for crystalline tetranactin complexed with K^+, Na^+, and Rb^+.[6] The mean cation–carbonyl oxygen distance is only slightly less than the mean cation–ether oxygen distance in the K^+ and Rb^+ complexes of tetranactin (Table I), but it is some 0.4 Å smaller in the Na^+ complex. This suggests that the positions of the ether oxygens may be limited by steric factors in the Na^+ complex.

In contrast, a recent X-ray study of the tetranactin–NH_4^+ complex[7] reports hydrogen bonding between the NH_4^+ ion and the tetrahydrofuran ether oxygens of tetranactin [Fig. 1(d)]. The cation–ether oxygen distance is $\sim$ 0.12 Å smaller than the cation–carbonyl oxygen distance; the NH_4^+ protons are aligned on the ether oxygen atoms (and at about 75° to the C=O bond). The NH_4^+–ether hydrogen bonds may account for the great stability of the nonactin–NH_4^+ complex, as observed in extraction experiments.[1]

Equilibrium constants for nactin complexation have been obtained from studies of the extraction of alkali salts from aqueous to nonpolar bulk phases[1] and from proton magnetic resonance studies.[3] The selectivity sequence for nonactin is found to be $NH_4^+ > K^+ > Rb^+ > Cs^+ > Na^+ > Li^+$. As noted by Eisenman et al.,[1] the measurement of intrinsic binding constants with extraction experiments requires the assumption that the solution conformations of the various cation complexes are basically identical (i.e., "isosteric"). The test of this assumption is one of the motivations of the present work.

In a previous paper,[9] we reported a Raman spectroscopic study of uncomplexed nonactin, monactin, dinactin, trinactin, and tetranactin in the solid state and CCl_4, $CHCl_3$, CH_3OH, and 4:1 (v/v) $CH_3OH/CHCl_3$ solution. Comparison with model compounds permitted the identification of most spectral features. The conformation of crystalline monactin was found to be similar to that of uncomplexed nonactin and tetranactin (whose atomic coordinates are known),[10,11] while dinactin and trinactin were found to have a second, distinct, crystal structure. In contrast, the solution spectra of uncomplexed nonactin, monactin, and dinactin were similar. The solution conformation is evidently relatively open, allowing the formation of hydrogen bonds between solvent molecules and nactin ester carbonyl groups.

In the present work, we extend this study to the complexes of nonactin, monactin, and dinactin with Na^+, K^+, Rb^+, Cs^+, Tl^+, NH_4^+, NH_3OH^+, $C(NH_2)_3^+$, and Ba^{++}. Spectra of the monovalent complexes were obtained both in 4:1 (v/v) $CH_3OH/CHCl_3$ solution and in the solid state. Depolarization ratios were measured in solution. Some of our data on nonactin complexes have been reported in preliminary notes;[12,13] our results indi-

TABLE I
Summary of X-Ray Data[a]

Nactin	Cation	Z	Space Group	$M^+ \ldots O{=}C$	$M^+ \ldots O_C^C$	Reference
Nonactin	—	8	order–disorder structure	—	—	10
Nonactin	Na^+	4	$C2/C$	2.42	2.77	8
Nonactin	K^+	4	$Pnna$	2.81	2.81	5
Tetranactin	—	4	$C2/c$	—	—	29
Tetranactin	Na^+	8	$C2/c$	2.435	2.820	6
Tetranactin	K^+	4	$P2_1/n$	2.789	2.893	6
Tetranactin	K^+	8	$C2/c$	2.774	2.874	6
Tetranactin	Rb^+	4	$P2_1/n$	2.909	2.940	6
Tetranactin	NH_4^+	4	$P2_1/n$	3.010	2.894	7
Tetranactin	Ba^{++}	8	$P2_1/a$	—	—	29
Tetranactin	Cu^{++}	8	$P2_1/a$	—	—	29

[a] Note: Z = number of nactin molecules/unit cell. The fifth and sixth columns give the mean distances (Å) between the enclosed metal ion (M^+) and the carbonyl (O=C) and ether (C—O—C) oxygens.

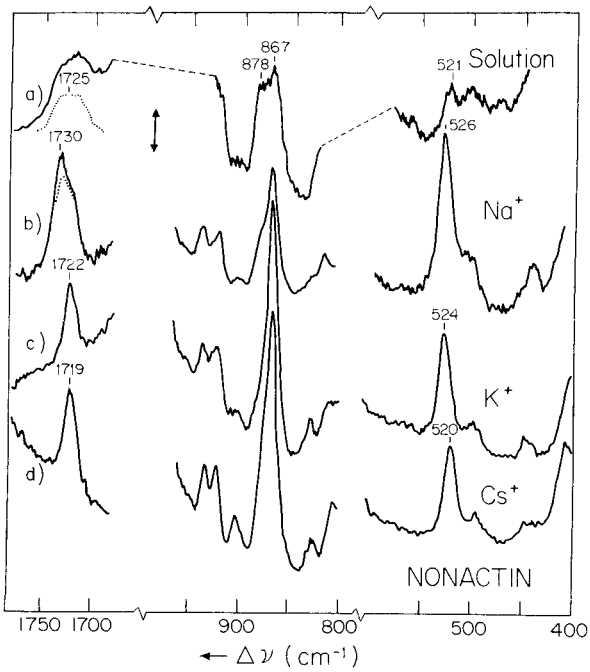

Fig. 2. Raman spectra of (a) uncomplexed nonactin and its (b) Na^+, (c) K^+, and (d) Cs^+ complexes in 4:1 (v/v) $CH_3OH/CHCl_3$. Vertical arrow represents (a), (b) 100 counts/sec, (c), (d) 300 counts/sec, except [(b), 800–950 cm^{-1}] 300 counts/sec. Scanning speed 30 cm^{-1}/min, slit width ~4 cm^{-1}, incident power 100–140 mW, and incident wavelength (a) 5145 Å, (b)–(d), 4880 Å. Solvent peaks obscure the intervening spectral regions.

cated that the cation–nactin ester carbonyl interaction is primarily electrostatic.

Our basic objective is to use Raman spectroscopy to study molecular conformation and molecular interactions in the cation complexes of the nactins. Since Raman spectroscopy can be applied both to solutions and to crystals, we are able to compare our results with the detailed structural information provided by X-ray diffraction on solid-state systems and to extend such results to the investigation of nactin conformations in solution.

METHODS AND MATERIALS

Raman spectra were measured using a SPEX Ramalog 4 double-grating monochromator system and the 4579, 4880 or 5145 Å line of a Spectra Physics Model 164-03 argon ion laser. Samples were held in Kimax glass capillaries mounted perpendicularly to the scattering plane; the polarization vector of the incident laser light was also perpendicular to the scattering plane. Laser powers of 20–100 mW (crystals) or 50–200 mW (solutions),

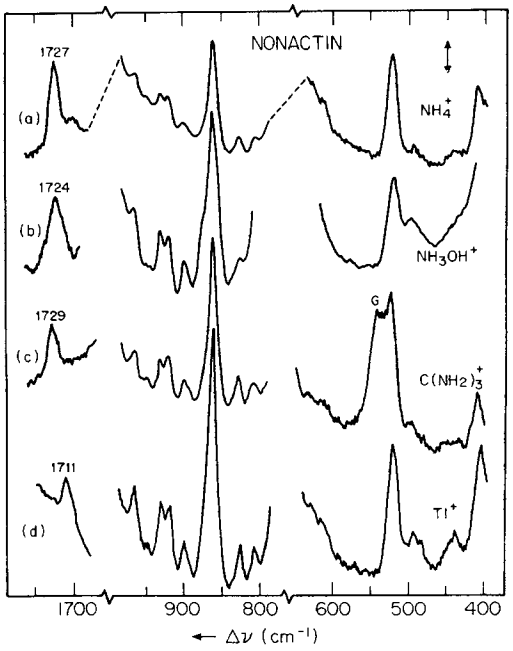

Fig. 3. Raman spectra of the (a) NH_4^+, (b) NH_3OH^+, (c) $C(NH_2)_3^+$, and (d) Tl^+ complexes of nonactin in 4:1 (v/v) $CH_3OH/CHCl_3$. Vertical arrow represents 300 counts/sec, except [(a), 800–1000 cm^{-1}] 500 counts/sec, [(c), 800–1000 cm^{-1}] 100 counts/sec, and [(d), 400–1000 cm^{-1}] 100 counts/sec. Scanning speed 30 cm^{-1}/min, slit width ~5 cm^{-1}, incident power 80–140 mW, and incident wavelength 4880 Å, except [(a), 400–600 and 1650–1750 cm^{-1}] 4579 Å.

scanning speeds of 30–60 cm^{-1}/min, and a spectral resolution of 5 cm^{-1} were used.

Polarization effects were studied using a polarization analyzer placed between the sample and the polarization scrambler, which was permanently mounted in front of the monochromator entrance slit.

In what follows, spectra of Raman scattered light with polarization parallel and perpendicular to that of the incident beam will be referred to as the "polarized" and "depolarized" spectra, respectively (hereafter denoted "$\|$" and "$\perp$", respectively). One can then assign each Raman peak a polarization ratio $\rho \equiv I_\perp/I_\|$, where $I_\perp$ and $I_\|$ are the intensities observed in the $\perp$ and $\|$ spectra, respectively. Under nonresonant conditions, ρ can never exceed $\frac{3}{4}$. If $\rho = \frac{3}{4}$, the peak is said to be "depolarized;" if $\rho = 0$, "polarized;" and if $0 < \rho < \frac{3}{4}$, "partially polarized."[14] Occasionally, peaks (labeled "D" in Tables IM–VM*) are more clearly observed in the depolarized spectrum ($\perp$) than in the polarized spectrum ($\|$). This is not a

* Tables IM–VM, detailing the spectral characteristics of nonactin, monactin, and dinactin complexes in solution, and monactin crystalline, and dinactin crystalline complexes have been stored in a microfiche repository. Readers wishing to obtain copies of these tables may do so by writing to Manager, Journal Production Department, John Wiley & Sons, Inc., 605 Third Avenue, New York, N.Y. 10016.

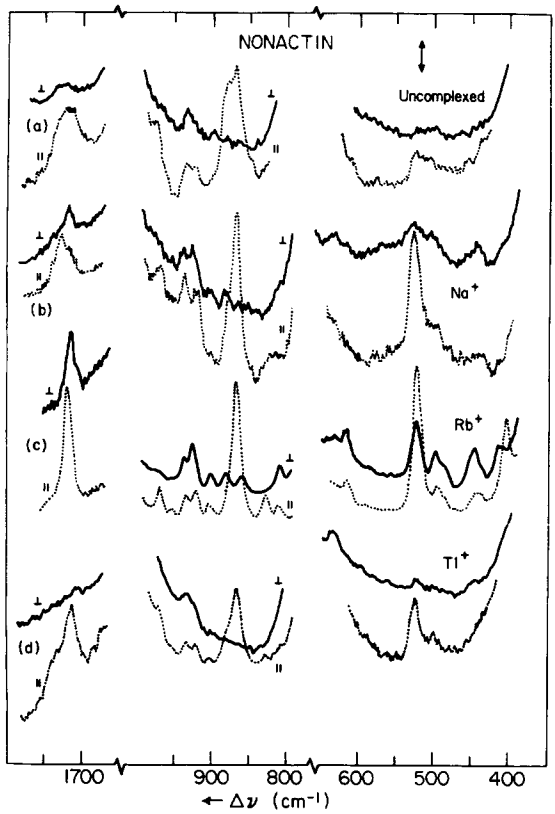

Fig. 4. Polarized (∥) and depolarized (⊥) Raman spectra of (a) uncomplexed nonactin in 2:1 (v/v) $CH_3OH/CHCl_3$ nd its (b) Na^+, (c) Rb^+, and (d) Tl^+ complexes in 4:1 (v/v) $CH_3OH/CHCl_3$. (Uncomplexed nonactin is less soluble in CH_3OH than its complexes.) Vertical arrow represents 100 counts/sec, except: [(b), ⊥, 1650–1750 cm^{-1}] 30 counts/sec, [(b), ∥, 400–600 cm^{-1}] 140 counts/sec, [(b), ∥, 800–1000 cm^{-1}] 200 counts/sec, [(c), ∥, 400–600, 1650–1750 cm^{-1}, and (c), ⊥, 800–1000 cm^{-1}] 300 counts/sec, [(d), ∥, 800–1000 cm^{-1}] 300 counts/sec, and [(c), ∥, 800–1000 cm^{-1}], 1000 counts/sec. Scanning speed 30 cm^{-1}/min, slit width ~5 cm^{-1}, incident power ~250 mW, and incident wavelength 5145 Å, except (a) 4880 Å. Note that the depolarized spectra were generally taken with a higher instrumental sensitivity than the polarized spectra.

violation of the requirement $\rho \leq 3/4$; rather this effect arises because a decrease in the intensity of a polarized band in the ⊥ spectrum may unmask nearby depolarized bands.

The nonactin was the gift of Dr. B. Stearns of the Squibb Institute for Medical Research (Princeton, New Jersey); the monactin and dinactin were gifts of Dr. H. Bickel and Dr. K. Scheibli of Ciba-Geigy, Ltd. (Basel, Switzerland). Crystals of tetranactin–Ba^{++} were kindly provided by Dr. K. Ando and Dr. Y. Nawata of Chugai Pharmaceutical Company, Ltd. (Tokyo, Japan). All were used without further purification. The solvent mixture of 4:1 (v/v) $CH_3OH/CHCl_3$ was chosen to provide sufficient solubility of

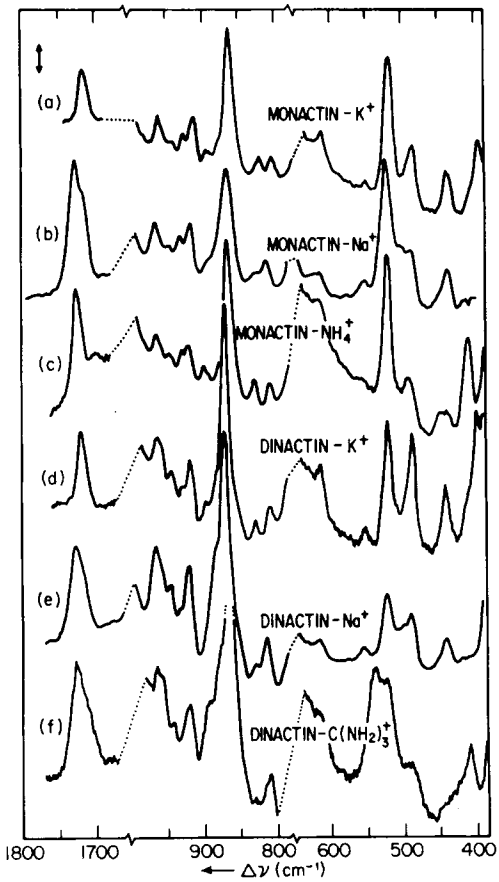

Fig. 5. Raman spectra of the (a) K^+, (b) Na^+, and (c) NH_4^+ complexes of monactin, and the (d) K^+, (e) Na^+, and (f) $C(NH_2)_3^+$ complexes of dinactin in 4:1 (v/v) $CH_3OH/CHCl_3$. The other complexes resemble the corresponding K^+ complex. Vertical arrow represents [(a)–(c), 400–600, 1650–1750 cm^{-1}] 300 counts/sec, [(a)–(c), 800–1000 cm^{-1}] 1000 counts/sec, [(d), (f), 400–600 cm^{-1}] 100 counts/sec, [(d), (f), 800–1800 cm^{-1})] 300 counts/sec, and (e) 1000 counts/sec. Notice that the relative intensity of the band near 525 cm^{-1} decreases in the series nonactin, monactin, and dinactin. Scanning speed 30 cm^{-1}/min, slit width ~4 cm^{-1}, incident power ~200 mW, incident wavelength (a)–(c) 5145 Å, (d)–(f) 4880 Å.

both the nactins and salts; it provided an unobstructed view of the 400–650, 800–975, and 1600–1800 cm^{-1} spectral regions. Solvents were spectroscopic grade or equivalent.

Solutions (usually 0.03 *M* nactin, 0.5 *M* salt) were prepared directly in capillaries and lightly centrifuged. Crystalline samples were obtained by letting the solvent slowly evaporate from the capillary, permitting the nactin–cation complexes to recrystallize in the presence of excess salt. The salts used were NaSCN, $NaNO_3$, KSCN, KNO_3, KCl, $RbNO_3$, RbCl, CsCl, $TlNO_3$, TlCl, NH_4SCN, NH_4NO_3, NH_3OHCl, $C(NH_2)_3Cl$, $Ba(SCN)_2$, and $Ba(ClO_4)_2$. The anions affected the formation constant of the observed

TABLE II
Representative Raman Spectra of Nactin Complexes in Solution[a,b]

K^+ Complex				Tl^+ Complex		
Nonactin	Monactin	Dinactin	Assignment	Nonactin	Monactin	Dinactin
401 P	399 P	400 P	skeletal bend, including O–C–C and O–C=O bend	(405)	406 P	404 P
	406 sh D					
409 P	(411) sh	(414) D				
445	442	444		441	442 B	442
496 p/0.4	488 p/0.3	488 p/0.2	tetrahydrofuran ring def	493 p/0.3	491 P	489 P
521 D						
524 P	522 p/0.2	521 p/0.1	ester C–O–C bend	521 p/0.1	520 p/0.2	519 P
	553 p/0.5	553 p/0.4				(551)
616	613	615	O–C=O out-of-plane bend	(614)	(612)	(613)
809 D	808	(807) D	methyl side chain and C–C stretch	807 P	810 p/0.2	807 p/0.4
813 P		811 P				
826 P	825 P	829 p/0.1		826 P	828 P	829 p/0.3
(857) D	(857B) D	(856) D	ester C–O–C sym stretch	(857) D	(B) D	
864 P	868 P	871 p/0.04		865 p/0.06	868 P	869 p/0.06
(877) D	(876) D	(883) sh	tetrahydrofuran C–O–C sym stretch	(873) sh, D	(B) D	(883) sh

897 D	895 D	(894) D	CH_3 rock (ip); C–C stretch	(897) D	895 D	896
902 P	901 P	899 P		900 p/0.5	901 P	
917 P	916					
922 D		920 p/0.4	ester skeletal	920 p/0.5	920	919 p
932	931	930	def	931	931	(926) D
(950)	(945)	944 p/0.3	CH_2 and CH_3 rock			
		960 p/0.1		(949)	(946)	943
966 p/0.1	964 p/0.1	967 p/0.2		966	966	966 p
					(1705) B,D	
				1711 P	1710 p/0.2	1710 P
(1718) D	(1716) D	(1718)D	C=O stretch			
1721.5 p/0.2	1720 p/0.2	1720.5 p/0.2				
				(1732) P[c]	(1734) P[d]	e

[a] Solvent 4:1 (v/v) $CH_3OH/CHCl_3$. B = broad, def = deformation, sh = shoulder, ( ) = weak, exact frequency uncertain. sym = symmetric; asym = asymmetric. P = strongly polarized (absent in ⊥ spectrum); p = partially polarized (e.g., p/0.3 indicates a depolarization ratio of 0.3). D = peak best observed in depolarized (⊥) spectrum (due to decrease in nearby polarized nonactin or solvent line). Frequencies given are for the unpolarized spectrum (∥ + ⊥). In the ester carbonyl stretch region, the total, ∥ and ⊥ spectra often differ significantly; the intensity ration of the largest ∥ and ⊥ C=O stretch peaks is given in lieu of a depolarization ratio.

[b] Similar spectra of the Na^+, Rb^+, Cs^+, NH_4^+, NH_3OH^+, and $C(NH_2)_3^+$ complexes are available in the microfilm edition (Tables IM–IIIM).

[c] After manual subtraction of the 1711 cm^{-1} peak and background.

[d] Not always observed.

[e] Polarized shoulder near 1734 cm^{-1} occasionally observed.

complexes, but not their spectra (except by adding anion peaks). Complexes of the nonspherical NH_3OH^+ and $C(NH_2)_3^+$ ions were included to help distinguish between steric and electrostatic effects.[12,13]

Samples of uncomplexed nactins could be stored indefinitely, but powders and solutions of some nactin complexes often exhibited spectral changes after storage at 4°C (cf. Appendix).

The model compounds 2,5-dimethyl tetrahydrofuran and ethyl acetate were used to help identify tetrahydrofuran and ester carbonyl vibrations, respectively. Additional information was obtained from samples of nonactinic acid and its diester (acetyl, methyl) derivative, which were kindly provided by Prof. G. Büchi (Department of Chemistry, M.I.T.).

RESULTS: SOLUTION SPECTRA

Our data are presented in Tables IM–IIIM; typical spectra are displayed in Figures 2–4 (nonactin), Figure 5 (monactin and dinactin), and Tables II and III. Our discussion of the data is organized by spectral region.

400–650 cm^{-1} Region

The spectra of the uncomplexed nactins in solution all show a weak, broad, unresolved band near 495 cm^{-1}, with a peak near 520 cm^{-1} ($\sim$ 521, 517, 515 cm^{-1} in nonactin, monactin, and dinactin, respectively) of comparable intensity. Complexation greatly enhances the intensity of the peak near 520 cm^{-1}, which becomes one of the most prominent features of the spectrum (Figs. 2–5). In the Tl^+ complexes, the polarization ratio ρ of the 520 cm^{-1} peak is substantially lower ($0 < \rho < 0.1$) than in the other complexes ($\rho \sim 0.2$).

In the monovalent cation complexes, the frequency of the 520 cm^{-1} peak decreases almost linearly with increasing ionic radius R, the only exception being the bulky $C(NH_2)_3^+$ ion. In the dinactin and monactin complexes, these frequencies are typically lower than in nonactin (Tables II, IM–IIIM). This region of the spectrum has been suggested[9,14–16] to contain C–O–C bend vibrations of ether and ester groups. The assignment to ester vibrations is supported by the dramatic change in the intensity of the 520 cm^{-1} peak upon complexation and by its sensitivity to substitution at the ^{11}C position.

The broad 502 cm^{-1} band of uncomplexed nonactin shifts to 495 cm^{-1} upon complexation (except in the Na^+ complex in which it remains near 502 cm^{-1} as a broad shoulder on the intense 526 cm^{-1} peak). The 502 cm^{-1} peak is moderately polarized in nonactin ($\rho \sim 0.4$) and its monovalent complexes ($0.3 < \rho < 0.5$). The frequency of this band is systematically lower in monactin complexes (487–493 cm^{-1}) and dinactin complexes (488–489 cm^{-1}). The Tl^+ complex bands have the lowest polarization ratios.

Upon complexation, additional weak nactin bands are usually observed

TABLE III
Representative Raman Spectra of Nactin Crystalline Complexes[a,b]

K^+ Complex		Ba^{++} Complex			
Monactin	Dinactin	Monactin	Dinactin	Tetranactin	Assignment
145 sh	(144) sh				
(157) sh		167			
	(~174)			173	
180		203			OC–O Torsion (?)
	(253)	250		252	
(273)			287		
298	295	305	302	299	
	319				
323	328	323	327 sh		skeletal bend
				(343)	(including ester)
	368	347			
386	386	384	385	387	
401	400				
(414) sh	413	416	413		C–C–C and C–C=O
		(434)	426	431	skeletal bend
445	445	447		449	
				472	
490	490	490 B	(486)	484	
501	497		495		tetrahydrofuran ring def.
		510	511	513	
526	524				ester C–O–C bend
557	556			545	
615	615	(613)			ester def +
				623	C=O out-of-plane bend
			634		
		643			
685	683			680	
		698	698		C=O in-plane bend
708	706			704	

TABLE III (*continued*)

K^+ Complex		Ba^{++} Complex			
Monactin	Dinactin	Monactin	Dinactin	Tetranactin	Assignment
750				755	
764	765				CH_2 rock/twist
	809	807	806	811	methyl side chain
813		817	816		C–C stretch
828	831				
	(847) sh	(847)	850		ester C–O–C
(862) sh		863	863	863	sym. stretch
870	869	(874) sh			
		(883) sh	887	887	tetrahydrofuran C–C–C sym. stretch
897	893	890 sh			CH_3 in-plane rock + C–C stretch
		(905)			
921	921	917	919		
932	929	929	929	c	ester skeletal def
948	946	(948) B	944		
			953	954	
966	965	(966)	964	967	CH_2 rock
(989) sh	(990)				CH_3 rock
	(1001)				
1014	1014				CH_3 def
	1025	1020	c	1022	C–C stretch
d	d				
(1057) sh	1057	1061 B	1057	1060	tetrahydrofuran C–O–C
1087	1085	1085			asym stretch
		1094	1092	1094	ester O–C–C asym stretch
1117	1118			1110	
1124 sh	(1121) sh	1122	1123		
1142	1142	1141 sh		1141	

		1157	1155	1157	
1161	1161				Asym CH_3 rock
(1169) sh	(1168) sh	1168	1167		
1197	1197	1197	1195	1202	ester C–O–C asym stretch
(1213) sh	1211				
(1232)	1231	(1235) sh	1230	1231	CH_2 twist/rock
1251	1251	1249	1245 B		
		(1274)		1264 B	
1281	(1278) sh			1282 B	
1287	1288	1285	1285		
1309	1308	1313	1314	1308	CH_2 Wag
1319	(1323) sh			1321	CH def
1335	1335				
(1344) sh		(1340–	1347		
1360	1359	1354) B	1363	1365	CH_3 sym bend
(1387)	(1385) sh	1387	1387	1387	
1397	1399				
		1415	1410		C^{10} CH_3 asym def
(1438) sh	(1436) sh			1434	CH_2 bend
1452	1455	1447	1447	1449	CH_3 asym def
1461	(sl)	1464	1460	1464	
		1695	1692	1694	C=O stretch
1719	1719	1714	1714	1714	
	(2735)				
2748					combination frequencies
2768	(2767)				
(2843) sh			2843		CH_2 sym stretch
			2873		
2884	2883		2882	2884	CH_3 sym stretch
		2890		2898	
	2906	2911			
2913	2918		2916	2916	CH stretch
2925					

TABLE III (*continued*)

K^+ Complex		Ba^{++} Complex			
Monactin	Dinactin	Monactin	Dinactin	Tetranactin	Assignment
2938	2941	2940		2938	CH_2 asym stretch
			2947	2947	
	(2961)				
2974	2977	2973	2975		CH_3 asym stretch
2987	(2987) sh	2985		2985	
				(3008)	

[a] Powders of KSCN complexes crystallized from 4:1 (v/v) CH_3OH:$CHCl_3$. Monactin and dinactin–$Ba(SCN)_2$ complexes were precipitated from 4:1 (v/v) CH_3OH:$CHCl_3$; the tetranactin–$Ba(ClO_4)_2$ complex was a single crystal. B= CH_3OH:$CHCl_3$; the tetranactin–$Ba(ClO_4)_2$ complex was a single crystal. B = broad, sh = shoulder, sl = slant, ( ) = weak, frequency uncertain; sym = symmetric, asym = asymmetric, def = deformation.

[b] Similar tables for the monactin Na^+, Rb^+, Cs^+, NH_4^+, and Tl^+ complexes and the dinactin Na^+, Rb^+, NH_4^+, $C(NH_2)_3^+$ and Tl^+complexes are shown on microfilm (Tables IVM and VM). Data in IVM indicate that the monactin NH_3OH and $C(NH_2)_3^+$ complexes dissociate during evaporation and crystallization. Raman spectra of the uncomplexed nactins are tabulated in Ref. 9.

[c] Solvent or anion peaks obscure this region.

[d] Very large, presumably extraneous, peaks appear in this region, making measurements of nactin modes difficult (see Appendix).

near 405, 445, 615, and (in the higher nactins) 555 cm^{-1}; the 405 cm^{-1} band is not observed in Na^+ complexes. The exact frequency of the 405 cm^{-1} band is difficult to measure due to interference from the neighboring solvent peak, but it appears to increase in the series $K^+ < Rb^+ < Cs^+ < NH_4^+ < C(NH_2)_3^+$. The band is highly polarized in all nactins ($0 < \rho < 0.1$), but an additional depolarized component appears ~5 cm^{-1} higher in the $\perp$ spectra of some nactin complexes.

The unresolved singlet observed near 443 cm^{-1} in the K^+, Rb^+, Cs^+ complexes can be decomposed into a polarized (~440 cm^{-1}) and depolarized (~447 cm^{-1}) doublet in some nactin NH_4^+, NH_3OH^+, and $C(NH_2)_3^+$ complexes. Normal mode calculations on aliphatic polyesters[15] predict O-C=O bending vibrations near 430–460 cm^{-1}; ethyl acetate has a weak peak near 442 cm^{-1}. This mode and the neighboring 405–410 cm^{-1} band could also represent O–C–C skeletal bend.[15] The 443 cm^{-1} band is too weak to be observed in the uncomplexed nactins, which is consistent with the observed enhancement of the intensity of the other ester peaks (520, 867, 1720 cm^{-1}) upon complexation.

Despite interference from an adjacent polarized solvent line, the depolarized peak near 615 cm^{-1} appears at approximately the same position in all of the nactin complexes. The 615 cm^{-1} peak is not observed in solutions of uncomplexed nonactin or monactin (it appears as a weak shoulder in uncomplexed dinactin). It may correspond to ester carbonyl out-of-plane bending vibrations (611 cm^{-1} in ethyl acetate), although a weak 613 cm^{-1} shoulder appears in spectra of 2,5-dimethyltetrahydrofuran.

800–975 cm^{-1} Region

In uncomplexed nonactin, this region is dominated by an intense, highly polarized doublet at 867, 878 cm^{-1}. In contrast, the 878 cm^{-1} peak of nactin complexes is very weak and depolarized while the intensity of the ~867 cm^{-1} peak (which remains polarized) is greatly enhanced. An additional weak peak appears near 857 cm^{-1} in the complexes. Due to the intensity of the 867 cm^{-1} peak, the 857 and 878 cm^{-1} peaks can usually only be seen in the depolarized spectra (cf. Fig. 4(c); Tables IM–IIIM). (The 878 cm^{-1} shoulder is visible in unpolarized ($\parallel + \perp$) spectra of most dinactin complexes.)

For a given nactin, the frequencies of the 867, 878 cm^{-1} peaks are nearly independent of the complexed ion (being ~1 cm^{-1} higher for the lighter alkali ions). As discussed in Ref. 9, these peaks probably correspond to ester and ether C–O–C symmetric stretch vibrations, respectively. The frequency of the 864 cm^{-1} peak of nonactin complexes increases to ~868 cm^{-1} for monactin and 869 cm^{-1} for dinactin.

Uncomplexed nactins display a faint band near 898 cm^{-1} which becomes appreciably more intense upon complexation. A single, depolarized peak is seen in spectra of the Na^+ complexes. A close doublet, composed of a strong polarized component (whose frequency decreases in the series

nonactin–dinactin) and a weaker depolarized component (~3–5 cm^{-1} lower in frequency) is seen in the other complexes. We previously[9] assigned this vibration to coupled methyl in-plane rock/C–C stretch vibrations on the basis of previously published studies of hydrocarbon chains.[17–19]

Spectra of uncomplexed nonactin and monactin display a doublet near 922, 931 cm^{-1}. Upon complexation, the lower peak downshifts ~2 cm^{-1} in most complexes; its frequency is consistently lower for Na^+, K^+, and Rb^+ than for the other ions. Upon complexation, the 931 cm^{-1} peak shifts up ~1 cm^{-1} in nonactin and down ~1 cm^{-1} in monactin. In contrast, uncomplexed dinactin displays a singlet near 925 cm^{-1}, which shifts to 921 cm^{-1} upon complexation. Some dinactin complexes also show a weak shoulder near 931 cm^{-1}. These modes may represent coupled ester skeletal deformation and CH_3 rock, as does the 922, 944 cm^{-1} doublet of ethyl acetate.

There is a weak polarized peak near 970 cm^{-1} in spectra of the uncomplexed nactins, assigned previously[9] to combined methyl rock, C–C stretch, and/or skeletal deformation. A similar peak appears near 966 cm^{-1} in spectra of nactin complexes.

1700–1750 cm^{-1} Region

This spectral region contains the ester carbonyl stretch frequency.[20,21] In previous notes,[12,13] we have shown that the frequency of this vibration is particularly sensitive to details of the interactions between ester carbonyl groups and complexed cations. Since there are several ester carbonyl groups, there will be several ester carbonyl stretch modes, some of which may be degenerate in frequency. If the carbonyl groups are arranged around the cation in a tetrahedron, as is seen in X-ray crystallographic data,[5–8] the local symmetry around the cation will be T_d. From the usual symmetry rules,[22] the nine atoms in this local group (four C, four O, one cation) will contribute a total of nine modes: two A_1 modes, two E modes (doubly degenerate), one F_1 mode (triply degenerate), and four F_2 modes (triply degenerate). The A_1, E, and F_2 modes are Raman active (the A_1 modes being polarized); only the F_2 modes are infrared active. The C=O and O. . .cation stretch coordinates give rise to eight spectral lines; by comparison with the normal modes of CH_4, these are seen to be the two A_1 modes and two triply degenerate F_2 modes. In one A_1 mode and one triply degenerate F_2 mode, C=O stretch will dominate, leading to spectral lines in the 1700 cm^{-1} region. In the other two modes, low-frequency (<500 cm^{-1}) O. . .cation stretch dominates; such modes have been observed in the infrared spectrum of valinomycin.[23]

In uncomplexed nonactin, the carbonyl stretch peak appears as a single broad band near 1725 cm^{-1}, which is seen in the polarized spectrum as a 1732 cm^{-1} band (with a 1716 cm^{-1} shoulder) and in the depolarized spectrum as a 1720, 1733 cm^{-1} doublet. A broad polarized doublet appears near 1718, 1732 cm^{-1} in spectra of uncomplexed monactin and dinactin. The

splitting of the polarized and unpolarized peaks may arise from hydrogen bonding to the solvent; that hydrogen bonding reduces carbonyl stretch frequencies has previously been observed in simple esters[24] and depsipeptides.[25,26]

Upon complexation with ions other than Na^+ and Tl^+, the broad band seen in the uncomplexed nactins near 1725 cm^{-1} sharpens into an intense, highly polarized peak with a depolarized shoulder located 2–5 cm^{-1} lower in frequency. The intensity of the depolarized shoulder is $\sim 1/5$ that of the polarized peak. The polarized component corresponds to the fully symmetric stretch A_1 mode (i.e., all four carbonyl groups stretching in phase) while the depolarized line corresponds to the F_2 mode. As discussed below, the A_1 mode is the most useful for studies of the antibiotic–cation interaction.

The nactin–Na^+ complexes are the only ones to display a distinct doublet ($\sim$1720, 1730 cm^{-1}) in the unpolarized ($\| + \perp$) spectrum. The shape of this peak might at first suggest that some free nactin is present; however, spectra taken in 0.5 *M* and 2.0 *M* NaSCN have the same line shape, indicating that the nactin molecules are all complexed. The 1720 cm^{-1} peak is depolarized; the 1730 peak is polarized and, therefore, corresponds to the symmetric A_1 mode.

Unlike complexes with other ions, the nactin–Tl^+ complex shows a single, intense, highly polarized peak at an exceptionally low frequency ($\sim$1710 cm^{-1}). There is no depolarized component (except perhaps near 1705 cm^{-1} in the monactin complex), but there is a weak, polarized band near 1735 cm^{-1}.

Additional *weak* polarized peaks appear near 1705 cm^{-1} in the NH_4^+ and $C(NH_2)_3^+$ complexes, except in dinactin–$C(NH_2)_3^+$ (in which it appears near 1714 cm^{-1}).

SOLID-STATE SPECTRA

Raman spectra were obtained of crystalline cation complexes of monactin and dinactin. These were obtained by evaporating to dryness nactin solutions containing an excess of salt. Our data are presented in Tables III, IVM, and VM. Typical Raman spectra are presented in Table III and Figures 6 and 7. Efforts to crystallize nactin–NH_3OHCl complexes produced samples whose spectra closely resemble those of the uncomplexed nactins [compare Figs. 6(a) and 7(b)]. Apparently, the forces which stabilize the nactin–NH_3OH^+ complex in solution do not effectively compete with the interactions which stabilize the NH_3OHCl and uncomplexed nactin crystal lattices. Similarly, solid-state samples of the dinactin–CsCl and the monactin–$C(NH_2)_3Cl$ complexes could not be obtained.

In general, the Raman spectra of the crystalline complexes show considerably more detail than the solution spectra because: 1) no spectral regions are obscured by solvent lines; 2) the peaks are narrower than in solution spectra, permitting more detailed observation of substructure; and

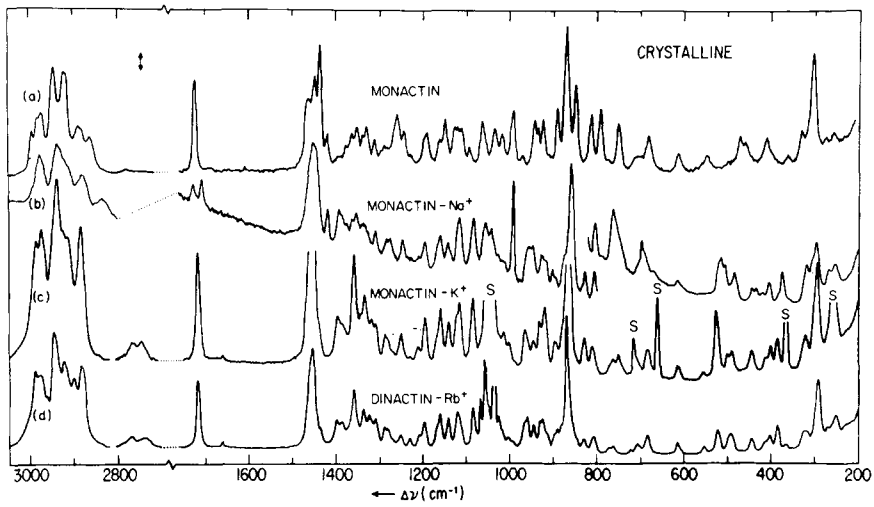

Fig. 6. Raman spectra of (a) crystalline monactin, (b) the monactin–Na^+ complex, (c) the monactin–K^+ complex, and (d) the dinactin–Rb^+ complex. The nactin complexes were obtained by total evaporation of solutions containing an excess of salt. "S" denotes a residual solvent peak. Vertical arrow represents (a), (c) 100 counts/sec, (b), (d) 300 counts/sec, except between 2800–3100 cm^{-1} where (a), (c) 300 counts/sec, (b), (d), 1000 counts/sec. Scanning speed 30 cm^{-1}/min, slit width ~4 cm^{-1}, incident power (a) 90 mW, (b) ~40 mW, incident wavelength (a), (b) 5145 Å, (c), (d) 4579 Å.

3) contact forces between adjoining molecules in the solid cause frequency shifts and line splittings.

For example, in the different complexes, the deformation modes of the tetrahydrofuran ring (near 490 cm^{-1} in solution) are differently affected by crystallization. The singlets observed in solutions of monactin–K^+, $C(NH_2)_3^+$ are split into doublets (~12 cm^{-1} separation) in the solid state. The ~490 cm^{-1} peak of the Na^+ complexes shifts ~5 cm^{-1} downward, while that of the dinactin–Rb^+, Tl^+ complexes shifts ~4 cm^{-1} upward. Similarly, the ~440 cm^{-1} bands of the Na^+ complexes [Figs. 5(b) and 5(e)] are split into clearly resolved doublets in the solid state (Fig. 6(b), Table IVM).

The ester deformation band seen near 522 cm^{-1} in nactin solutions is downshifted considerably in crystalline dinactin–Na^+, monactin–Na^+, and monactin–Cs^+ (15, 8, 5 cm^{-1}, respectively). In the other crystalline complexes, the solid-state frequencies of this mode are shifted *upward* 2–5 cm^{-1}. Similarly, the peak near 932 cm^{-1}, which may represent ester skeletal deformations, is shifted downward only in the crystalline dinactin–Na^+, and monactin–Na^+, monactin–$C(NH_2)_3^+$, and monactin–Cs^+ complexes. These results, and the anomalously high carbonyl stretch frequency of the crystalline monactin–Cs^+ complex (upshifted 4 cm^{-1}) suggest that crystallization may slightly affect the structure of some complexes.

Other anomalies are observed for the largest and smallest cations. For example, the dinactin–$C(NH_2)_3^+$ complex is characterized by the absence of a 444 cm^{-1} peak, a 7 cm^{-1} downshift in the 385 cm^{-1} peak, and the co-

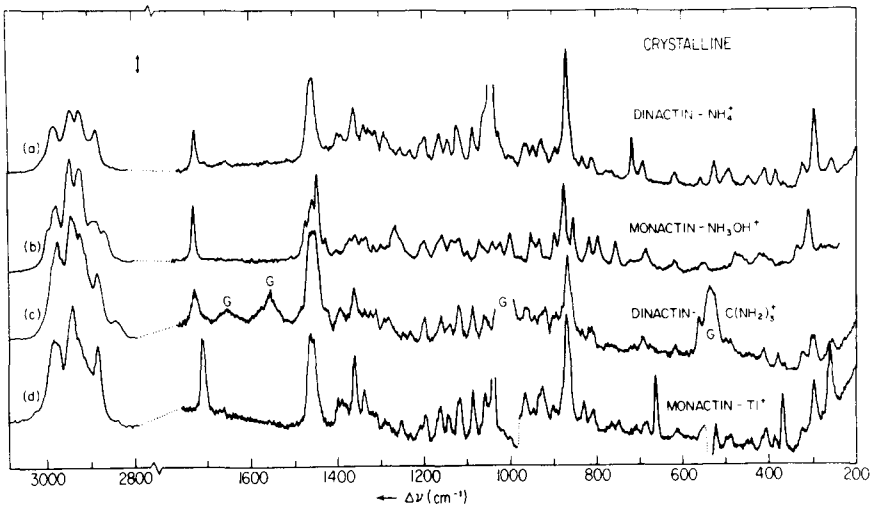

Fig. 7. Raman spectra of crystalline (a) dinactin–NH_4^+ complex, (b) monactin crystallized from a solution containing a tenfold excess of NH_3OHCl (uncomplexed), (c) dinactin–$C(NH_2)_3^+$ complex, and (d) monactin–Tl^+ complex. Vertical arrow represents 100 counts/sec, except between 2800–3100 cm^{-1} (300). Scanning speed 30 cm^{-1}/min, slit width ~4 cm^{-1}, incident power (a), (b) ~40 mW, (c), (d) ~100 mW, incident wavelength (a) 5145 Å, (b), (c) 4880 Å, (d) 4579 Å. The monactin–NH_3OHCl complex dissociated upon crystallization. Guanidinium peaks are denoted by G.

alescence of the doublet near, 1394 cm^{-1}. Similarly, solid-state samples of dinactin–Cs^+, dinactin–$C(NH_2)_3^+$ and monactin or dinactin–NH_3OH^+ could not be obtained.

Pronounced crystalline effects are also seen in the carbonyl stretch region. The unresolved 1720, 1729 cm^{-1} doublet of the monactin–Na^+ complex in solution [Fig. 5(b)] is split into a distinct 1708, 1727 cm^{-1} doublet in the solid state. A close 1720, 1729 cm^{-1} doublet of the dinactin–Na^+ complex is similarly resolved (1709, 1733 cm^{-1}) in the solid state (Tables IIIM and VM). Upon crystallization, the carbonyl stretch frequencies ν_{CO} of the monactin–Rb^+, Cs^+, and Tl^+ complexes shift −3, +4, −1.5 cm^{-1}, respectively; those of the dinactin–K^+, Rb^+, and Tl^+ complexes shift −1.5, −1.5, −2 cm^{-1}, respectively. In all other cases in which the comparison can be made, ν_{CO} is shifted 1 cm^{-1} or less downward. As in solution, ν_{CO} is apparently the same for both monactin and dinactin complexes (Fig. 12).

Although the CH_2, CH_3 stretch region (2800–3000 cm^{-1}) of the uncomplexed nactins was found to be sensitive to crystal packing,[9] it is essentially the same for all the crystalline complexes except NH_4^+, in which the 2923, 2942 cm^{-1} peaks are of equal intensity [Fig. 7(a)]. However, the nactin–NH_4^+ samples are fully complexed; notice, for example, that they lack the ~2866, 2884 cm^{-1} doublet seen in the uncomplexed solid-state mixture of monactin and NH_3OHCl [Figs. 7(a) and (b)]. The NH_4^+ complexes also lack the subtle substructure typical of this region in the other complexes.

On occasion, variable, intense lines appear near 1000–1050 cm^{-1} in

spectra of crystalline dinactin complexes; they appear to be artifacts (see Appendix).

DISCUSSION

In general, two types of information may be obtained from our data. First, cation-dependent changes in the frequency and line shape of particular spectral lines may give information about cation–nactin interactions. In particular, the ester carbonyl stretch frequency ($\sim$1720 cm^{-1}) gives information about the cation–carbonyl interaction. Similarly, spectral changes can provide information about the interaction of nactin complexes with their environment (crystalline forces, solvents, etc.). Second, line shapes and polarization measurements can provide information about the conformation and symmetry of the nactin complex. Such data provide a test of isostericity—the assumption that the complexes of different cations are basically similar in conformation. Comparison of spectra taken in the solid state and in solution may indicate the extent to which X-ray diffraction studies on the crystalline complexes can be used to interpret the behavior of the nactins in solution.

Nactin–Cation Interactions

The symmetric ester carbonyl stretch mode (which may readily be distinguished from the other ester carbonyl stretching modes by its great intensity and complete polarization) is found to be a particularly useful probe of the cation–nactin carbonyl interaction. Since the carbonyl group is usually in close contact with the cation, one might expect that a force which causes the nactin ring to expand to accommodate a larger cation would perturb the carbonyl stretch mode. Such a perturbation might be expected to be proportional to the force distorting the nactin ring, and thus be simply related to the ionic radius of the enclosed cation. That is, although the primary nactin–cation interaction is electrostatic, *differences* in the interaction in different cation complexes could have a simple, steric explanation. This would suggest a simple dependence of the corresponding ester carbonyl stretch frequency ν_{CO} on cationic radius R. Figure 8 plots ν_{CO} as a function of R for eight different cation complexes. For the polyatomic cations, R is the average of the four N. . .O distances, as taken from X-ray data[7] and simple models (Fig. 9). For the Na^+ and K^+ complexes, X-ray structural data give better values for the cation–oxygen distances than those afforded by the simple model; these values are indicated by the crosses in Figures 8 and 10.

As is seen in Figure 8, ν_{CO} is not a simple function of R, at least for the polyatomic cations. In particular, the Cs^+, NH_3OH^+, and $C(NH_2)_3^+$ ions have approximately the same average Cs^+ . . .O or N. . .O distances, but quite different stretch frequencies ν_{CO}. (While it is, of course, possible to change the definition of the average radius R, in order for ν_{CO} of the

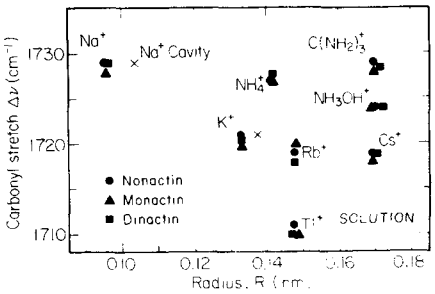

Fig. 8. Ester carbonyl stretch frequency ν_{CO} as a function of ionic radius for complexes of nonactin (●), monactin (▲), and dinactin (■) in 4:1 (v/v) $CH_3OH/CHCl_3$. For Na^+ and K^+ complexes, the ionic radius and the cavity radius (as defined by the ion-oxygen distances) are not the same. The crosses indicate cavity radii (Refs. 5 and 8). Notice that the Cs^+, NH_3OH^+, and $C(NH_2)_3$ complexes display different frequencies ν_{CO} even though the ions are of similar size.

$C(NH_2)_3^+$ complexes to fit on the same curve as the alkali complexes, it would be necessary for the average radius of $C(NH_2)_3^+$ to be *less* than that of K^+.)

A closer examination of Figure 8 indicates that ν_{CO} for the monoatomic alkali cations depends approximately on $1/R$. This suggests the possibility that ν_{CO} is being perturbed by cation–nactin carbonyl electrostatic interactions, rather than by contact between cation and nactin carbonyl. This hypothesis is tested in Figure 10, which plots ν_{CO} as a function of the electrostatic interaction energy U, as calculated from a simple model (Fig. 9). For most complexes, ν_{CO} is proportional to U. Note, in particular, the position of the Cs^+, NH_3OH^+, and $C(NH_2)_3^+$ complexes. These results indicate that the variation in the nactin–cation interaction between different cation complexes arises primarily from electrostatic, rather than steric, effects.

Some of the observed departures from the straight line of Figure 10 might be expected. The extraction coefficients of NH_4^+ and Tl^+ by nonactin (from an aqueous to a bulk organic phase) are anomalous.[1,27] The NH_4^+ ion is known, at least in tetranactin,[7] to hydrogen bond to the tetrahydrofuran rings. The nactin . . .Tl^+ interaction may also contain a nonelectrostatic contribution, namely, partially covalent bonds between the Tl^+ ion and the nactin carbonyl groups.[27] Finally, X-ray crystallographic measurements[6] on the nonactin–Na^+ complex show that steric interactions between the ester carbonyl oxygen atoms prevent them from coming in contact with the Na^+. The small deviation ($\sim$1 cm^{-1}) for the large Cs^+ cation may not be significant, since it is less than the uncertainty in the best position of the line (Fig. 10).

Induction Effect

The ionic selectivities of the five homologous nactins are not the same. Krasne and Eisenman have proposed[27] that these differences may arise

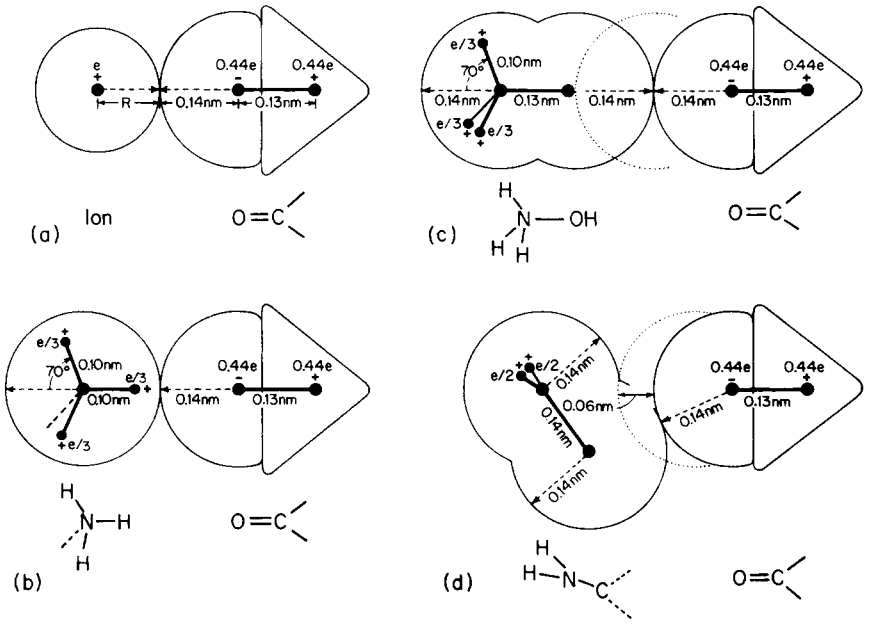

Fig. 9. (a) Model of Krasne and Eisenman[27] for the ion-carbonyl electrostatic interaction, showing the edges of the ion (radius R) and the oxygen (radius 0.14 nm) in contact. It is assumed that the nactin molecules are flexible and that the other ester carbonyl groups assume equivalent positions with respect to the cation. The indicated point charges are located at the nuclei (solid circles). The carbonyl charges are from the Krasne–Eisenman discussion of nonactin. (b) Modification of the Krasne–Eisenman model[27] to describe the interaction of an ester carbonyl group with amine protons, as in the NH_3OH^+ complex. In the NH_3OH^+ complex, one carbonyl group (c) interacts sterically with the hydroxyl group. The dotted circle indicates the position that the carbonyl group would take if the hydroxyl group were absent. In the $C(NH_2)_3^+$ complex, two carbonyl groups (d) interact sterically with the carbon atom of the cation; the dotted circle shows the position that the carbonyl oxygen would assume if the $C(NH_2)_3^+$ ion were absent. The other two carbonyl groups approach the hydrogens of one NH_2 directly as in (b). The other NH_2 groups of the $C(NH_2)_3^+$ cation extend into and out of the plane and are omitted for clarity. The electrostatic interaction energy U for the NH_3OH^+ and $C(NH_2)_3^+$ complexes was calculated for the sterically unhindered carbonyl groups (b) using the fractional charges shown in (c) and (d), respectively.

because the inductive effect of the additional ethyl groups in the higher nactins (cf. Fig. 1) increases the effective charge on the neighboring carbonyl groups. If ν_{CO} is sensitive to the electrostatic interaction energy U (as it appears to be), comparison of our measurements on nonactin, monactin, and dinactin may be used to test this proposal. In the higher nactins, an increase in the average charge separation would increase U for the affected carbonyl groups, leading either to a line splitting (if the effect were large enough) or to an increase in the average ν_{CO}.

Such effects are not seen. The carbonyl stretch peaks of monactin and dinactin complexes in solution (Fig. 5) are the same width as those of nonactin (Figs. 2–4). The values of ν_{CO} for the three nactins are almost

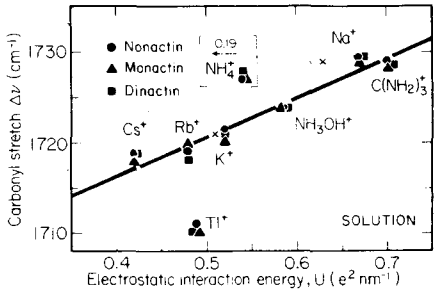

Fig. 10. Ester carbonyl stretch frequency ν_{CO} as a function of electrostatic interaction energy U for nonactin (●), monactin (▲), and dinactin (■) complexes in 4:1 (v/v) $CH_3OH/CHCl_3$. U is calculated by Coulomb's law for the charges and positions shown in figure 9, supplemented by available X-ray structural data. Crosses indicate values of U calculated with the aid of X-ray data rather than the simpler model of Figure 9. Compare the positions of the Cs^+, NH_3OH^+, and $C(NH_2)_3^+$ ions with those of Figure 8. Atomic coordinates obtained from X-ray diffraction, when combined with the formal charges of Figure 10(b), give a value $U = 0.19$ for the tetranactin-NH_4^+ complex.

identical (Fig. 10), and no systematic differences leading to a change of slope are seen. Although the average value of ν_{CO} for monovalent nonactin complexes is ~0.6 cm^{-1} higher than for monactin or dinactin, this would correspond (Fig. 10) to a ~3% *reduction* in the average electrostatic interaction energy U, which is the opposite of the effect suggested by Krasne and Eisenman.[27] The observed reduction in ν_{CO} could arise from changing the effective mass of the nactin molecule near the ester group (caused by replacement of methyl with ethyl groups). Furthermore, effective mass and inductive effects could fortuitously cancel.

Data for the crystalline complexes (Fig. 11) are similar to those found in solution (Fig. 10), except that the Cs^+ complex lies off the line defined by the Rb^+, K^+, NH_3OH^+, and $C(NH_2)_3^+$ ions. It is interesting that the line for the crystalline complexes has the same slope as the line for the solutions. This suggests that crystal interactions have about the same effect on ν_{CO} in all of these complexes.

Other Spectral Regions

Although the ~920 cm^{-1} (skeletal deformation) peaks of the nonactin and monactin complexes undergo a considerable change in intensity upon complexation, their frequencies increase only slightly with R or U either in solution (Fig. 11) or in the solid state. However, the frequency of the K^+ complexes is anomalously low in solution. The frequencies of the dinactin complexes vary somewhat erratically from one ion to another, but are typically 1–3 cm^{-1} higher than the corresponding frequencies of nonactin or monactin.

Except for the solid-state Na^+ complex, the frequency of the ~520 cm^{-1} (ester C–O–C bend) peak decreases monotonically with R both in solution (Fig. 12) and in the solid state. That this regularity includes even the NH_4^+

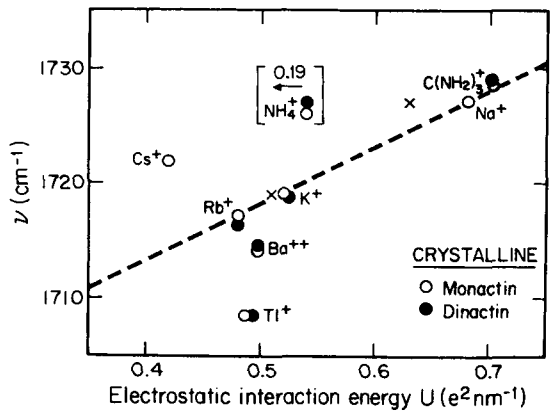

Fig. 11. Ester carbonyl stretch frequency ν_{CO} as a function of electrostatic interaction energy U for crystalline complexes of monactin (○) and dinactin (●). The results are similar to those obtained in solution (Fig. 10) except that Cs^+ and NH_3OH^+ now lie off of the line defined by the Rb^+, K^+, and $C(NH_2)_3^+$ ions (the line is roughly parallel to the line of Fig. 10).

ion (which forms hydrogen bonds with the nactin tetrahydrofuran oxygens) and Tl^+ ion (which may interact partially covalently with the nactins) suggests that the frequency of this mode is sensitive primarily to steric effects, rather than to any specific details of the nactin–cation interaction.

Conformation and Isostericity

One of the central assumptions in interpreting the chemical properties of the nactins has been that their monovalent cation complexes are isosteric, i.e., "that the overall size and shape of the complex, as well as its externally viewed charge distribution, are the same for all cations."[27] With this assumption, the nactin-solvent interactions are the same for all of the monovalent cation complexes, permitting one to use bulk-phase partition coefficients to study the intrinsic ionic selectivities of the nactins.[1,27] A related problem is the determination of what conformations a complex assumes in different environments. X-ray diffraction measurements have been made on many nactin complexes in the solid state,[5–8,28,29] but similar X-ray measurements are not possible on the solutions.

Raman spectroscopy may be used both in the solid state and in solution, permitting a study of the relation between the conformations determined by X-ray measurements in the solid state and the conformations present in solution. Conformational differences are reflected in differences in the line frequencies and polarizations observed in Raman experiments. (However, Raman spectra are not directly very sensitive to nactin complex–solvent interactions.) Thus, Raman measurements can probe isostericity in solution: if the conformations of the various nactin–cation complexes are different, they are unlikely to be isosteric. These spectra, except for Na^+ and Tl^+, are highly similar (Figs. 2–5, Tables IM–IIIM),

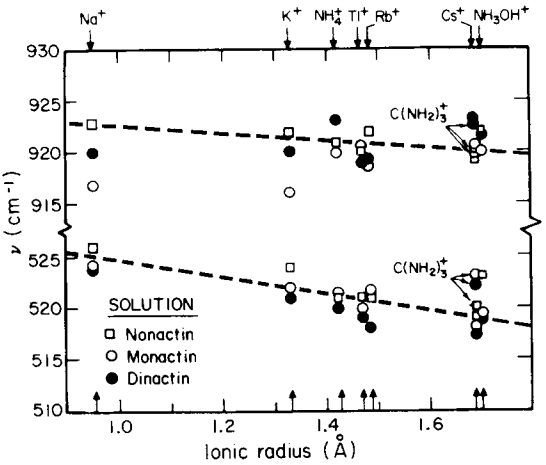

Fig. 12. The frequencies of the 529 cm^{-1} (C–O–C bend) and 920 cm^{-1} (skeletal deformation) peaks of nonactin (□), monactin (○), and dinactin (●) monovalent complexes in 4:1 (v/v) $CH_3OH/CHCl_3$ solution, plotted as a function of ionic radius R. Complexes are identified by the atomic radii of their cations (arrows at top of figure). For clarity, the $C(NH_2)_3^+$ data points are identified separately in the figure.

although there are a few minor differences in the NH_4^+, NH_3OH^+, and $C(NH_2)_3^+$ complexes. The Na^+ complexes: 1) lack a 405 cm^{-1} band; 2) show no shift in the 520 cm^{-1} peak upon complexation; 3) exhibit an increase (rather than a decrease) in the polarization of the 520 cm^{-1} peak; 4) retain a prominent shoulder near 878 cm^{-1}; and, most importantly, 5) display a ~1720, 1730 cm^{-1} doublet in the ester carbonyl stretch region. This suggests that the Na^+ complex is not isosteric to the other alkali complexes, a result not unexpected from X-ray data and structural chemical considerations. Because the oxygen atoms have a sterically imposed distance of closest approach, a Na^+ ion (R = 0.095 nm) is appreciably too small to touch all four nactin carbonyl oxygen atoms simultaneously.

The spectrum of the Tl^+ complex is also anomalous. In particular, the ester carbonyl peak (~1710 cm^{-1}) is fully polarized, no activity being apparent in the depolarized ($\perp$) spectrum. This could arise if: 1) the Raman activity of the asymmetric mode were too weak to be observed, or 2) the symmetry of the carbonyl groups about the enclosed ion were different than in the other complexes. Case 1) would imply that the spatial derivatives of the polarizability of the Tl^+ complexes were different than those of the other complexes, consistent with the presence of different (e.g., partially covalent) intramolecular bonding. In either case, the distribution of electronic charge around the Tl^+ ion differs from that around other cations. This implies (but does not prove) that the Tl^+ complex is not isosteric to the others.

The solutions of the complexes with NH_4^+, NH_3OH^+, and $C(NH_2)_3^+$ generally show a weak peak near 1705 cm^{-1}. This peak may represent a

further splitting of the coupled C=O cation modes by N–H stretch and other intracationic vibrations. The hydrogen bonding observed by Nawata et al.,[7] in the tetranactin–NH_4^+ complex may manifest itself in the anomalously high ν_{CO} (Fig. 10) in this complex. The lack of tetrahedral symmetry in the NH_3OH^+ and $C(NH_2)_3^+$ ions is not reflected in the Raman spectra of their complexes.

The solid-state spectra of the monactin and dinactin complexes are similar to each other and to their solutions. The solid-state Na^+ complexes display a sharp, fully resolved ~1709, 1730 cm^{-1} doublet. This suggests that the ester carbonyl groups of the Na^+ complex are very strongly coupled (X-ray studies on the monactin–Na^+ complex have previously suggested such a coupling).

Thus all the monovalent nactin complexes, except Na^+ and Tl^+, are conformationally similar in the solid state as well as in solution; it is reasonable to assume most of them are isosteric. Since solvation has little effect on the Raman spectra of the nactin complexes, the conformations adopted in the solid state and solution must be similar. This supports the use of available X-ray crystallographic data in elucidating the properties of the nactin complexes in solution.

NACTIN–BARIUM COMPLEXES

Nactin–Ba^{++} complexes are highly insoluble in 4:1 (v/v) $CH_3OH/CHCl_3$ and are immediately precipitated from solutions of uncomplexed nactins by the addition of excess $Ba(SCN)_2$. The bulk of the remaining solvent can be removed by prolonged drying. Our solid-state data are summarized in Figure 13. The tetranactin–$Ba(ClO_4)_2$ complex was the gift of Dr. K. Ando and Dr. Y. Nawata.

The Ba^{++} complexes resemble the crystalline Na^+ complexes in that the stretch vibrations of the coordinating nactin carbonyl groups are split into a sharp doublet of ~20 cm^{-1} separation (Figs. 6(b) and 13). However, the stretch frequencies of the Ba^{++} complexes are considerably (13–19 cm^{-1}) lower, indicative of unusual carbonyl–cation interactions. The increased electrostatic carbonyl–cation interaction could draw the carbonyl groups further inward, thereby decreasing the effective cavity size and making steric constraints more important for divalent ions than for the corresponding monovalent ions. Ester carbonyl stretch frequencies below 1700 cm^{-1} are rare, yet we find peaks at 1695 cm^{-1} in monactin–Ba^{++}, 1692 cm^{-1} in dinactin–Ba^{++} and 1694 cm^{-1} in tetranactin–Ba^{++}. This indicates unusually strong coupling between the carbonyl groups and the coordinated Ba^{++} ion.

The monactin–Ba^{++} and dinactin–Ba^{++} complexes also resemble the Na^+ complexes in having a sharp, isolated $^{10}C–CH_3$ deformation peak near 1415 cm^{-1} and a broad diffuse 1335–1365 cm^{-1} region (partially CH_3 wag). Similar features are also found in the uncomplexed nactins [Fig. 6(a)]. Since the nactin methyl groups point outward, they might be influenced

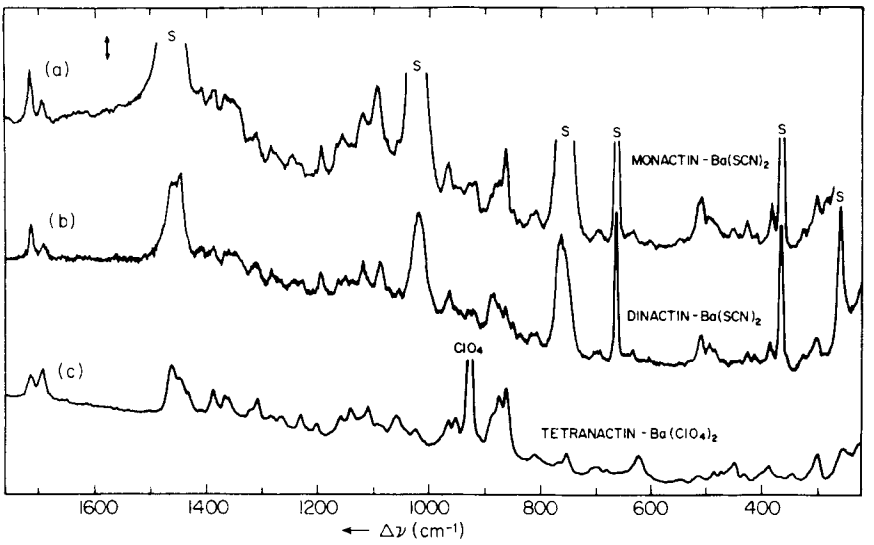

Fig. 13. Raman spectra of crystalline complexes of (a) monactin, (b) dinactin, and (c) tetranactin with Ba^{++}. The distinct splitting and low frequencies observed in the carbonyl stretch region contrast with the single bands observed in spectra of monovalent complexes other than Na^+ (Figs. 2–6). Vertical arrow represents (a), (b) 100 counts/sec, (c) 300 counts/sec. Scanning speed 30 cm^{-1}/min, slit width 4 cm^{-1}, incident power (a), (b) 100 mW, (c) 40 mW, incident wavelength (a) 4880 Å, (b) 5145 Å, (c) 4579 Å. Samples (a), (b) were precipitated from 4:1 (v/v) $CH_3OH/CHCl_3$; sample (c) was a single crystal.

by crystal packing; however, the space group of the tetranactin–Ba^{++} complex ($P2_1/a$) differs from that of tetranactin–Na^+ and uncomplexed tetranactin ($C2/c$). Unfortunately, similar data are not yet available for monactin and dinactin (tetranactin has no ^{10}C–CH_3 groups). The ester C–O–C bend of the nactin–Ba^{++} complexes resembles nactin–Na^+ by appearing near 510 cm^{-1} instead of 525 cm^{-1}.

The Ba^{++} complexes differ from all monovalent complexes (including Na^+) in several respects. The 860–890 cm^{-1} region (C–O–C stretch) is no longer dominated by the band near 860–870 cm^{-1} (which appears near 863 cm^{-1} as in nactin–Na^+). Instead, there are several peaks of comparable intensity (Fig. 13), one of which (883 cm^{-1} in monactin–Ba^{++}; 887 cm^{-1} in dinactin–Ba^{++}) is ~10 cm^{-1} lower than in the corresponding Na^+ complex. The 1100–1200 cm^{-1} region is more diffuse than in the monovalent complexes. Monactin–Ba^{++} lacks the 401–409 cm^{-1} peak of other monactin complexes; and dinactin–Ba^{++} lacks a peak near 444 cm^{-1}. Conversely, 634 cm^{-1} and 643 cm^{-1} peaks appear only in dinactin–Ba^{++} and monactin–Ba^{++}, respectively. Thus, the conformation of the nactin–Ba^{++} complexes may be closely related to that of the Na^+ complexes, but they are clearly not the same as the nactin complexes of the other monovalent cations. Figure 11 suggests that the nactin–Ba^{++} interaction includes steric, as well as electrostatic, factors.

APPENDIX

Some difficulty was caused by spectroscopic changes which take place over several weeks in some nactin crystalline complexes kept at 4°C. Intense spectral lines appear near 960, 1000–1040, 1360, 1385, 1640 cm^{-1} with few appreciable changes elsewhere in the spectrum. These new lines were not seen in uncomplexed crystalline nactins stored for up to one year under the same conditions. Solutions of the complexed nactins in 4:1 (v/v) $CH_3OH/CHCl_3$ (kept in sealed capillaries at 4°C) occasionally display a 1640 cm^{-1} line with <10% of the intensity seen in crystalline samples.

In a series of measurements in CH_2Cl_2 solution, a 1630 cm^{-1} peak often appeared within hours after the nactin powder was dissolved. Dilution of uncomplexed nonactin with CH_2Cl_2 (from 1.15 *M* to 0.02 *M*) had no effect on the ratio of the 1630 and 1720 cm^{-1} lines, suggesting that a hypothetical nonactin dimer is not responsible for the 1630 cm^{-1} peak. On addition of NH_4Cl and evaporation of the CH_2Cl_2, an apparently normal nonactin–NH_4^+ complex was formed, although the 1630 cm^{-1} peak was still present. We do not have a definitive interpretation for these effects, which we believe to be artifacts. Peaks at 1630, 1385, 1360, and 960 cm^{-1} are consistent with this effect arising from the solvolysis of nactin ester linkages to form a carboxylic acid residue and another, unspecified, group.

We refrained from using solution spectra in which the 1640 cm^{-1} line was prominent. For the crystalline spectra, this was not always possible; such cases are indicated by an asterisk in Tables IVM and VM.

Samples of the pure nactins were the generous gifts of Dr. B. Stearns (Squibb Institute for Medical Research) and Dr. H. Bickel and Dr. K. Scheibli (Ciba-Beigy, Ltd.); a sample of the tetranactin–Ba^{++} complex was kindly provided by Dr. K. Ando and Dr. Y. Nawata (Chugai Pharmaceutical Co., Ltd.). Prof. G. Buchi (M.I.T.) kindly provided a sample of nonactinic acid diester. The authors wish to thank Prof. G. Eisenman (UCLA), Prof. S. Krasne (UCLA), and Dr. K. J. Rothschild for useful conversations, and the late Miss J. Montfort for technical assistance. This project was supported in part by grants from the Research Corporation, and the National Heart and Lung Institute (R. W. Mann, principal investigator).

REFERENCES

1. Eisenman, G., Szabo, G., Ciani, S., McLaughlin, S. & Krasne, S. (1973) "Ion binding and ion transport produced by neutral lipid-soluble molecules," *Progress in Surface and Membrane Science*, vol. 6, Academic, New York.

2. Pretsch, E., Vašák, M. & Simon, W. (1972) *Helv. Chim. Acta* **55,** 1098–1103.

3. Prestegard, J. H. & Chan, S. I. (1969) *Biochemistry* **8,** 3921–3927; Prestegard, J. H. & Chan, S. I. (1970) *J. Amer. Chem. Soc.* **92,** 4440–4446.

4. Kyogoku, Y., Ueno, M., Akutsu, H. & Nawata, Y. (1975) *Biopolymers* **14,** 1049–1064.

5. Kilbourn, B. T., Dunitz, J. D., Pioda, L. A. R. Y Simon, W. (1967) *J. Mol. Biol.* **30,** 559–563.

6. Itaka, Y., Sakimaki, T. & Nawata, Y. (1972) *Chem. Letters (Japan),* 1225–1230.

7. Nawata, Y., Sakimaki, T. & Iitaka, Y. (1975) *Chem. Letters (Japan),* 151–154.

8. Dobler, M. & Phizackerley, R. P. (1974) *Helv. Chim. Acta* **57,** 664–674.

9. Phillies, G. D. J., Asher, I. M. & Stanley, H. E. (1975) *Biopolymers* **14,** 2311–2327.

10. Dobler, M. (1972) *Helv. Chim. Acta* **55,** 1371–1384.

11. Nawata, Y., Sakamaki, T. & Iitaka, Y. (1974) *Acta Crystallogr.* **B30,** 1047–1053.

12. Phillies, G. D. J., Asher, I. M. & Stanley, H. E. (1975) *Science* **188,** 1027–1029.

13. Asher, I. M., Phillies, G. D. J. & Stanley, H. E. (1974) *Biochem. Biophys. Res. Commun.* **61,** 1356–1362.

14. Tobin, M. C. (1971) *Laser Raman Spectroscopy,* Wiley-Interscience, New York, ch. 1, 2.

15. Tadokoro, H., Kobayashi, M., Yoshidome, H., Tai, K. & Makino, D. (1968) *J. Chem. Phys.* **49,** 3359–3373.

16. Colthup, N. B., Daly, L. H. & Wiberly, S. E. (1964) *Introduction to Infrared and Raman Spectroscopy,* Academic, New York, ch. 9, 10.

17. Snyder, R. G. & Schachtschneider, J. H. (1963) *Spectrochim. Acta* **19,** 85–115.

18. Snyder, R. G. & Schachtschneider, J. H. (1963) *Spectrochim. Acta* **19,** 117–155.

19. Snyder, R. G. & Schachtschneider, J. H. (1965) *Spectrochim. Acta* **21,** 169–195.

20. Thompson, H. W. & Torkington, P. (1945) *J. Chem. Soc.,* 640–645.

21. Katrizky, A. R., Lagowski, J. M . & Beard, J. A. T. (1960) *Spectrochim. Acta* **16,** 954–963.

22. Herzberg, G. (1945) *Infrared and Raman Spectroscopy of Polyatomic Molecules,* Van Nostrand Reinhold, New York, ch. 2, 3.

23. Ivanov, V. T., Kogan, G. A., Tulchinsky, V. M., Miroshinikov, A. I., Mikhaleva, I. T., Evstratov, A. V., Zenkin, A. A., Kostetsky, P. V., Ovchinnikov, Y. A. & Lokshin, B. V. (1973) *FEBS Lett.* **30,** 199.

24. Laato, M. & Isolato, R. (1967) *Acta Chem.* **21,** 2119–2130.

25. Rothschild, K. J., Asher, I. M., Anastassakis, E. & Stanley, H. E. (1973) *Science* **182,** 384–386.

26. Asher, I. M., Rothschild, K. J. & Stanley, H. E. (1974) *J. Mol. Biol.* **89,** 205–222.

27. Krasne, S. J. & Eisenman, G. (1973) in *Membranes, A Series of Advances,* vol. 2, G. Eisenman, Ed., Dekker, New York, p. 277.

28. Dobler, M., Dunitz, J. D. & Kilbourn, B. T. (1969) *Helv. Chim. Acta* **52,** 2573–2583.

29. Nawata, Y. & Ando, K. *Acta Crystallogr. (1972)* **B27,** 1680–1682.

Received January 27, 1976
Accepted June 16, 1976